

PDF hosted at the Radboud Repository of the Radboud University Nijmegen

The following full text is a publisher's version.

For additional information about this publication click this link.

<http://hdl.handle.net/2066/24957>

Please be advised that this information was generated on 2017-12-05 and may be subject to change.

Synchronized calcium spiking resulting from spontaneous calcium action potentials in monolayers of NRK fibroblasts

Albert D.G. de Roos¹, Peter H.G.M. Willems², Peter H.J. Peters¹,
Everardus J.J. van Zoelen¹, Alexander P.R. Theuvenet¹

Departments of ¹Cell Biology and ²Biochemistry, University of Nijmegen, Nijmegen, The Netherlands

Summary The correlation between the intracellular Ca^{2+} concentration ($[\text{Ca}^{2+}]_i$) and membrane potential in monolayers of density-arrested normal rat kidney (NRK) fibroblasts was investigated. Using the fluorescent probe Fura-2, spontaneous repetitive spike-like increases in $[\text{Ca}^{2+}]_i$ (Ca^{2+} spikes) were observed that were synchronised throughout the entire monolayer. Ca^{2+} spikes disappeared in Ca^{2+} -free solutions and could be blocked by the L-type Ca^{2+} channel antagonist felodipine. Simultaneous measurements of $[\text{Ca}^{2+}]_i$ and membrane potential showed that these Ca^{2+} spikes were paralleled by depolarisations of the plasma membrane. Using patch clamp measurements, action potential-like depolarisations consisting of a fast spike depolarisation followed by a plateau phase were seen with similar kinetics as the Ca^{2+} spikes. The action potentials could be blocked by L-type Ca^{2+} channel blockers and were dependent on extracellular Ca^{2+} . The plateau phase was predominantly determined by a Cl^- conductance and was dependent on intracellular Ca^{2+} . The presence of voltage-dependent L-type Ca^{2+} channels in NRK cells was confirmed by patch clamp measurements in single cells. It is concluded that monolayers of density-arrested NRK fibroblasts exhibit spontaneous Ca^{2+} action potentials leading to synchronised Ca^{2+} spiking. This excitability of monolayers of fibroblasts may represent a novel Ca^{2+} signaling pathway in electrically coupled fibroblasts, cells that were hitherto considered to be inexcitable.

INTRODUCTION

In electrically inexcitable tissues and cells, Ca^{2+} signaling is believed to be regulated via inositol trisphosphate (IP_3) formation, and subsequent Ca^{2+} release from intracellular stores, followed by Ca^{2+} entry from the extracellular medium via store-regulated Ca^{2+} -influx channels [1]. Furthermore, in monolayers of such non-excitable cells, it has been shown that the regenerative production of

inositol trisphosphate (IP_3) can induce Ca^{2+} waves that propagate slowly (2–20 $\mu\text{m}/\text{s}$) from cell to cell thereby providing a way for intercellular Ca^{2+} signaling in these cells via gap junctions [2]. Such intercellular propagation of Ca^{2+} signals can serve to co-ordinate multicellular responses to local stimuli.

In excitable cells, besides the above mechanism, Ca^{2+} may enter the cell when voltage-dependent Ca^{2+} channels are activated by depolarisations associated with action potentials. This Ca^{2+} signal can be amplified by Ca^{2+} -induced Ca^{2+} release (CICR) [3], thereby supplying sufficient Ca^{2+} for all-or-none responses [1]. Action potentials are caused in excitable cells by the regenerative opening of voltage-dependent ion channels. The action potential in axon and neuronal cells is caused by the regenerative opening of Na^+ channels [4]. In invertebrate and vertebrate muscle and in secretory cells, Ca^{2+} action potentials can also be generated by, in this case, opening

Received 12 June 1997

Revised 15 July 1997

Accepted 23 July 1997

Correspondence to: Dr Alexander P.R. Theuvenet, Department of Cell Biology, Toernooiveld 1, NL-6525 ED Nijmegen, The Netherlands

Tel: +31 24 365 2701; Fax: +31 24 365 2999

E-mail: atheuv@sci.kun.nl

of voltage-dependent Ca^{2+} channels [5]. Action potentials can be easily transduced to other cells via gap junctions, for which the propagation of the heart action potential is a classical example [6]. Also in other cells, transduction of action potentials via gap junctions has been shown to be involved in the co-ordination of cellular activities. For instance, synchronous Ca^{2+} oscillations in pancreatic islets are mediated by action potentials [7]. The increase in intracellular Ca^{2+} associated with action potentials provides a mechanism for long-range and fast co-ordinated Ca^{2+} signaling in excitable cells.

Although considered to be inexcitable, it has been reported that fibroblasts do possess voltage-dependent Ca^{2+} channels [8–12], but their function in these cells has so far been unclear. Fibroblasts can also be electrically coupled via gap junctions [13–17]. The presence of voltage-dependent Ca^{2+} channels and gap junctional intercellular communication could, in principle, enable these cells to generate intercellularly propagating action potentials, but such a mechanism has never been reported.

In the context of our interest in the molecular mechanisms underlying density-dependent growth arrest [18], we studied some biophysical parameters of density-arrested cells. Here, we report that monolayers of density-arrested NRK fibroblasts exhibit repetitive intracellular Ca^{2+} spikes that are synchronised throughout the entire monolayer. In contrast to density-arrested cells, quiescent NRK cells did not show spontaneous Ca^{2+} spikes. These spikes are paralleled by membrane potential spikes which result from spontaneously generated Ca^{2+} action potentials by the opening of voltage-dependent Ca^{2+} channels. The ability of density-arrested fibroblasts to exhibit Ca^{2+} action potentials represents a new mechanism for synchronised intercellular responses in fibroblasts and may be a mechanism underlying density-arrest.

MATERIALS AND METHODS

Cell culture

NRK fibroblasts (clone 49F) were seeded at a density of 1.0×10^4 cells/cm², and grown to confluence in Dulbecco's modified Eagle's Medium (DMEM; Gibco, Grand Island, NY, USA), supplemented with 10% newborn calf serum (Hyclone, Logan, UT, USA). Confluent cells were made quiescent by a subsequent 2–3 days' incubation in serum-free DF medium (DMEM, Ham's F12, 1:1) supplemented with 30 nM Na_2SeO_3 and 10 $\mu\text{g}/\text{ml}$ human transferrin, as described previously [19]. DF-medium is a cell culture medium which contains as main inorganic salts (in mM): 109.5 NaCl, 5.4 KCl, 1.8 CaCl_2 , 0.81 MgCl_2 , 44.0 NaHCO_3 , 1.0 NaH_2PO_4 , supplemented with essential nutrients such as glucose, amino acids and vitamins for optimal cell

growth. These quiescent cells were grown to density-arrest by an additional 48 h incubation with 5 ng/ml EGF (Collaborative Biomedical Products, Bedford, MA, USA) and 5 $\mu\text{g}/\text{ml}$ insulin (Sigma, St Louis, MO, USA).

Digital image fluorescence microscopy

Cells were grown on gelatin-coated glass coverslips and loaded with 5 μM Fura-2/AM (Molecular Probes, Eugene, OR, USA) in bicarbonate-buffered DF medium (pH 7.4) containing 0.01% (w/v) Pluronic F127 (Molecular Probes) for 30 min at room temperature. Since the monolayer integrity was lost after prolonged exposure to HEPES- or Tris-buffered solutions, media were bicarbonate-buffered and equilibrated with 5% CO_2 to a pH of 7.4. After loading, the cells were washed with DF medium for 30–90 min at room temperature. The cells were then placed in a perfusion chamber with a volume of 800 μl and were perfused with DF medium of indicated pH during the entire experiment at a rate of 1 ml/min at RT. In Ca^{2+} -free experiments, CaCl_2 was omitted from the medium and 1 mM EGTA was added. For membrane potential experiments, 75 nM of the bisoxonol DiBAC₄(3) (Molecular Probes) was present in the perfusion medium during the experiment. Excitation wavelengths were 340 and 380 nm for intracellular Ca^{2+} measurements with Fura-2 and 490 nm for the membrane potential experiment with DiBAC₄(3). Excitation filters were mounted in a motor-driven rotating wheel. The fluorescence emission was monitored at 492 nm. An epifluorescent 40 \times magnification oil immersion objective was used, which gave the opportunity to a simultaneous monitoring of around 100 cells. Occasionally, a 10 \times objective was used, which allowed monitoring of more than 1000 cells simultaneously. Dynamic video imaging was carried out using the MagiCal hardware and Tardis software of Joyce Loebel (Tyne and Wear, UK) as described previously [20]. In most experiments, 340/380 ratio signals were calculated directly after the experiment using the Tardis software. The discrete and limited ratio values that this software generates, resulted in some digital noise, which only reflects the limitations of the software. Additional intracellular Ca^{2+} measurements were performed on a conventional spectrofluorimeter (SPF-500, Aminco, Silver Spring, MD, USA) at an excitation wavelength of 340 nm and an emission wavelength of 480 nm.

Voltage and current clamp measurements

For whole cell patch clamp studies, cells were perfused with DF medium (pH 7.4) at a rate of 1 ml/min at room temperature. Conventional whole cell patch clamp methods were used. Pipettes were filled with a high K^+ , Tris-buffered solution (in mM: 25 NaCl, 120 KCl, 1 CaCl_2 ,

1 $MgCl_2$, 10 Tris, 3.5 EGTA, pH 7.4). An EPC-7 patch clamp amplifier (List, Darmstadt, Germany) and CED software (Cambridge Electronic Design Limited, Cambridge, UK) were used to acquire data. In ion substitution experiments, DF-medium was made from scratch and Na^+ and Cl^- were replaced by N-methyl-D-glucamine and gluconate, respectively. Since monolayers of NRK cells are electrically well-coupled [17], there is electrical access from the patched cell to neighbouring cells. Therefore, the measured membrane potential will be an average of many coupled cells and only the intracellular components of the patched cell are washed out. In this way, reliable membrane potential measurements could be performed for over 2 h.

For single cell patch clamp measurements, confluent NRK cells were trypsinised and replated in serum-containing DMEM. Whole cell patch clamp experiments were performed 2–4 h after attachment of the cells to the culture dish at room temperature. Extracellular medium consisted of (in mM): 10 $BaCl_2$, 92.5 TEA-Cl, 1 $MgCl_2$, 10 glucose, 10 *bis*-Tris-propane (BTP, Sigma), pH 7.4). Pipettes were filled with a solution containing (in mM): 105 CsCl, 3.5 EGTA, 1 $MgCl_2$, 200 μM Mg-ATP (Sigma), 10 BTP, pH 7.4. Cell capacitance and series resistance compensation was performed in these experiments.

Chemicals

Nifedipine, tetrodotoxin and octanol were from Sigma, bradykinin was from Boehringer (Mannheim, Germany), BAY K8644 was from Calbiochem (San Diego, CA, USA), BAPTA/AM was from Molecular Probes. Felodipine was a gift of Astra Hässle AB (Möln dal, Sweden).

RESULTS

Synchronous Ca^{2+} spikes in monolayers of density-arrested NRK fibroblasts

In our laboratory, NRK cells are usually grown to confluence in the presence of serum after which they are serum-deprived and become quiescent. When these quiescent cells are subsequently treated with epidermal growth factor (EGF) as the only growth stimulating polypeptide, the cells undergo one additional cell cycle before they undergo density-dependent growth inhibition or density-arrest [19]. In the present study, dynamic video imaging was performed on monolayers of such density-arrested NRK cells, loaded with the fluorescent probe Fura-2, to simultaneously monitor the cytosolic free Ca^{2+} concentration ($[Ca^{2+}]_i$) in large numbers of cells (approximately 100). Figure 1 shows that these cells exhibit spontaneous, repetitive transient increases in $[Ca^{2+}]_i$ (' Ca^{2+} spikes') that were synchronised

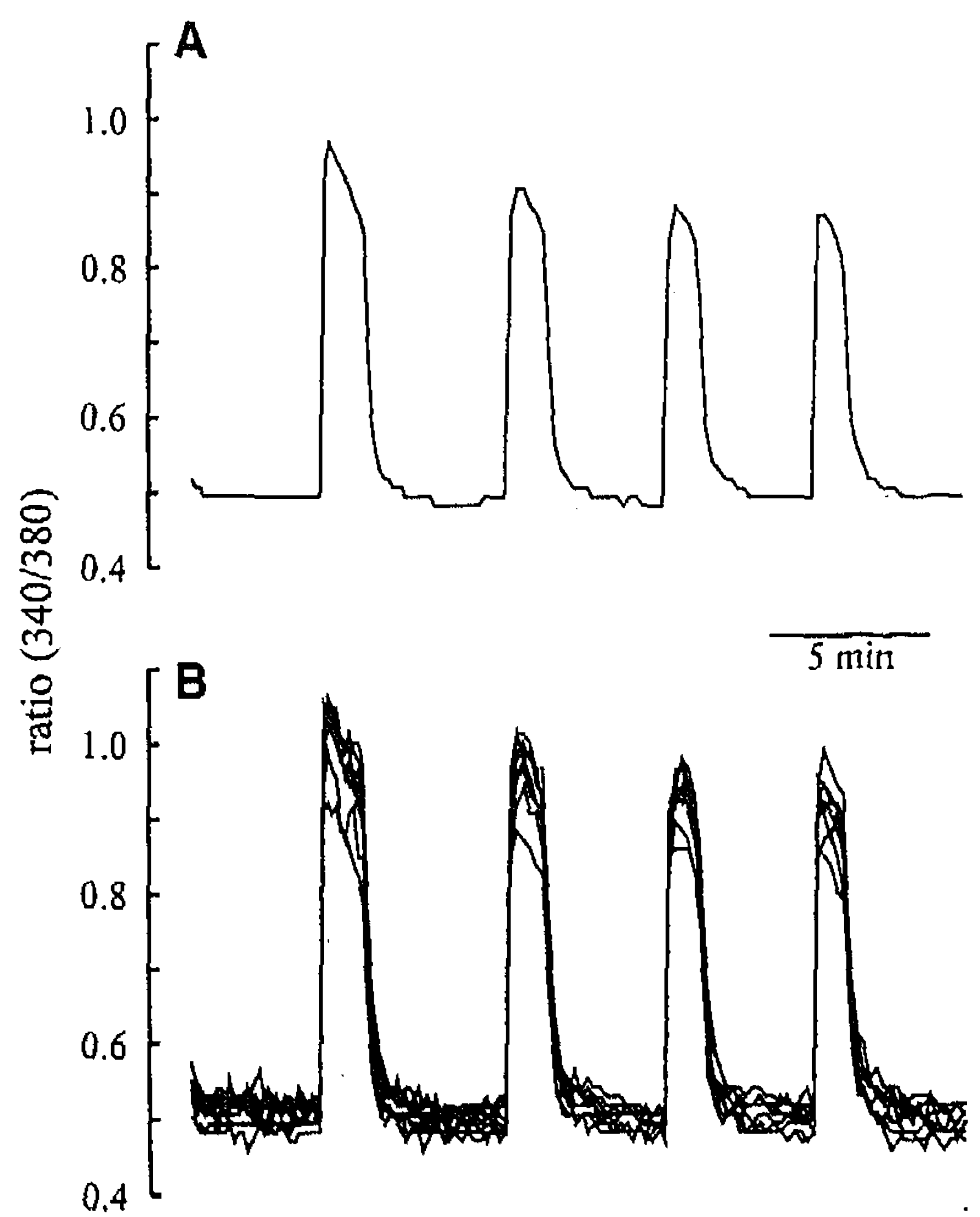


Fig. 1 Spontaneous synchronous repetitive increases in intracellular Ca^{2+} in monolayers of NRK fibroblasts. **(A)** The average increase in $[Ca^{2+}]_i$ of about 100 cells forming part of a density-arrested monolayer of NRK fibroblasts. **(B)** The response of seven randomly chosen individual cells from the cells taken from (A). Cells were continuously perfused with bicarbonate-based buffer with a pH of around 8.2. Cells were loaded with Fura-2 in order to measure the $[Ca^{2+}]_i$.

in all cells. In Figure 1A, the averaged response of all 100 cells is shown, whereas in Figure 1B the Ca^{2+} response is shown in 7 individual cells, which were randomly picked from all the measured cells. These results indicate that the $[Ca^{2+}]_i$ increased virtually simultaneously in all cells. The increase in $[Ca^{2+}]_i$ in each spike was comparable to that evoked by optimal concentrations of bradykinin, a potent Ca^{2+} -releasing agent in NRK cells (see also Fig. 5B). Ca^{2+} spikes consisted of a fast rising phase, followed by a slowly declining plateau phase, which could last more than 1 min, after which Ca^{2+} levels quickly declined to resting values. This decline was also synchronised in all cells.

The frequency and probability of occurrence of the spontaneous repetitive Ca^{2+} spikes were highly variable between individual cell cultures. In physiological DF media equilibrated to a pH of 7.4, about 50% of the density-arrested monolayers showed occasional Ca^{2+} spikes with a low frequency, whereas about 25% of these cultures showed repetitive Ca^{2+} spikes. The rest of the monolayers did not show spontaneous Ca^{2+} spikes. However, the probability of occurrence of the repetitive spikes could be increased to about 50% by omitting CO_2 from the bicarbonate-buffered medium, resulting in a pH

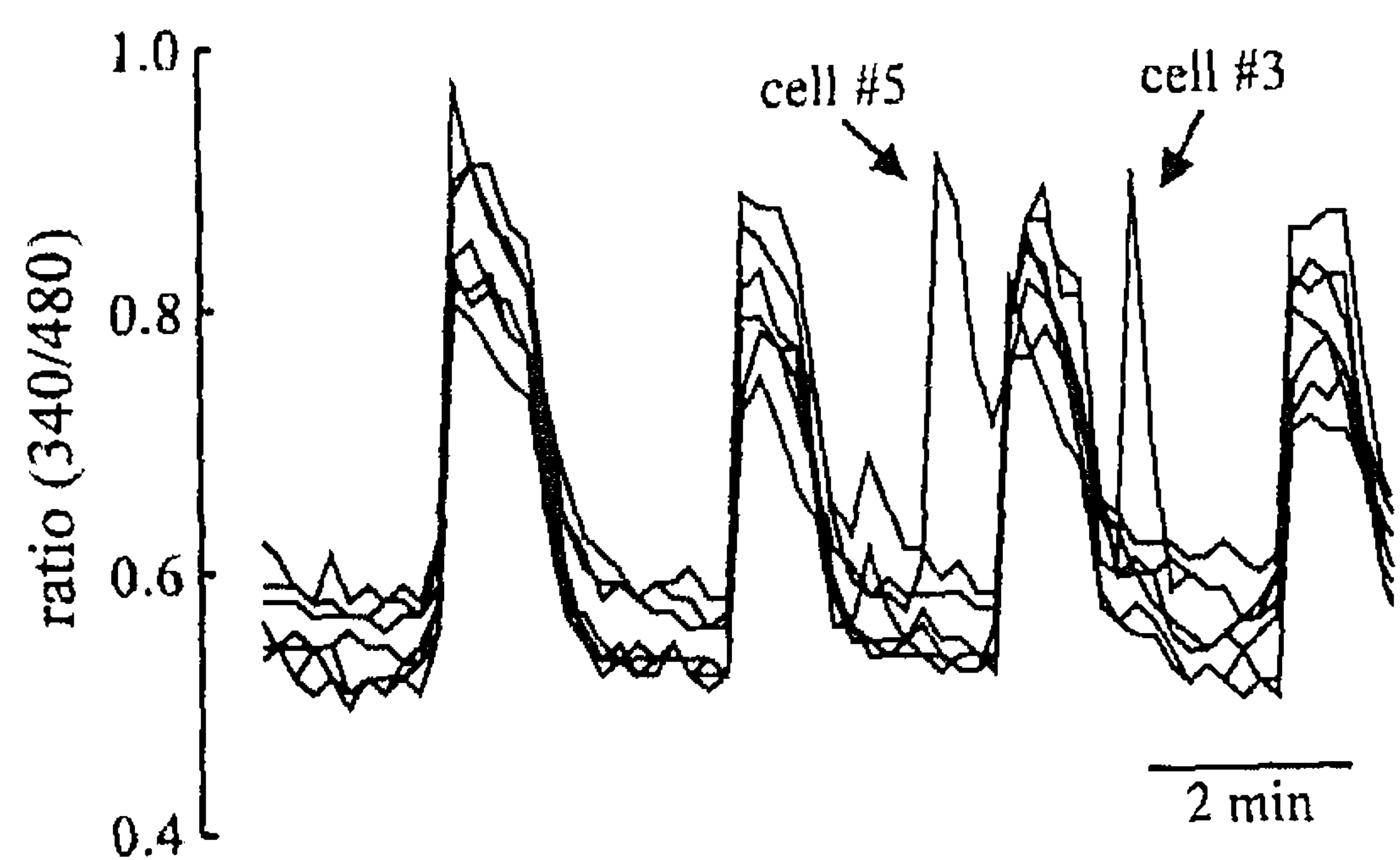


Fig. 2 Asynchronous increases in intracellular Ca^{2+} in cells that exhibited spontaneous Ca^{2+} spikes. The response in $[\text{Ca}^{2+}]_i$ is shown in six neighbouring cells that displayed synchronous Ca^{2+} spikes. Two of the cells (#3 and #5) show, apart from the synchronous increases, also an asynchronous increase in $[\text{Ca}^{2+}]_i$.

increase to approximately 8.2. Synchronous Ca^{2+} spikes had the same shape in normal (pH 7.4) and high pH, although the duration of the spikes was longer in high pH medium (not shown). Because we were interested in the molecular mechanisms underlying the Ca^{2+} spikes, we routinely used medium with a high pH to increase their incidence. Under these conditions, frequency ranged from values as low as 1 or 2 transients per 20 min to values as high as 10 transients per 20 min. Of note, spontaneous Ca^{2+} spikes were never seen in serum-deprived, quiescent NRK cells.

The role of intracellular Ca^{2+} in the induction of spontaneous Ca^{2+} spikes

The role of intracellular Ca^{2+} as a possible trigger for the synchronous Ca^{2+} spikes was investigated by looking at Ca^{2+} concentrations in individual cells. Beside the synchronous Ca^{2+} spikes, occasionally asynchronous increases in $[\text{Ca}^{2+}]_i$ were seen. Figure 2 is an example of such a case and shows the individual Ca^{2+} responses of a group of 7 adjacent cells within a monolayer that exhibited synchronous Ca^{2+} spikes. Two cells in the group of 7 cells displayed an asynchronous Ca^{2+} increase. This Ca^{2+} increase was not followed by an increase in $[\text{Ca}^{2+}]_i$ in neighbouring cells. These results clearly demonstrate that Ca^{2+} increases in individual cells do not necessarily trigger synchronous Ca^{2+} spikes and suggest that Ca^{2+} itself is not significantly transferred between cells.

Synchronisation of the Ca^{2+} spikes throughout the entire monolayer

In the experiments shown above, only about 100 cells in the monolayer were analysed. By using a 10 \times objective instead of a 40 \times objective, we were able to analyse more

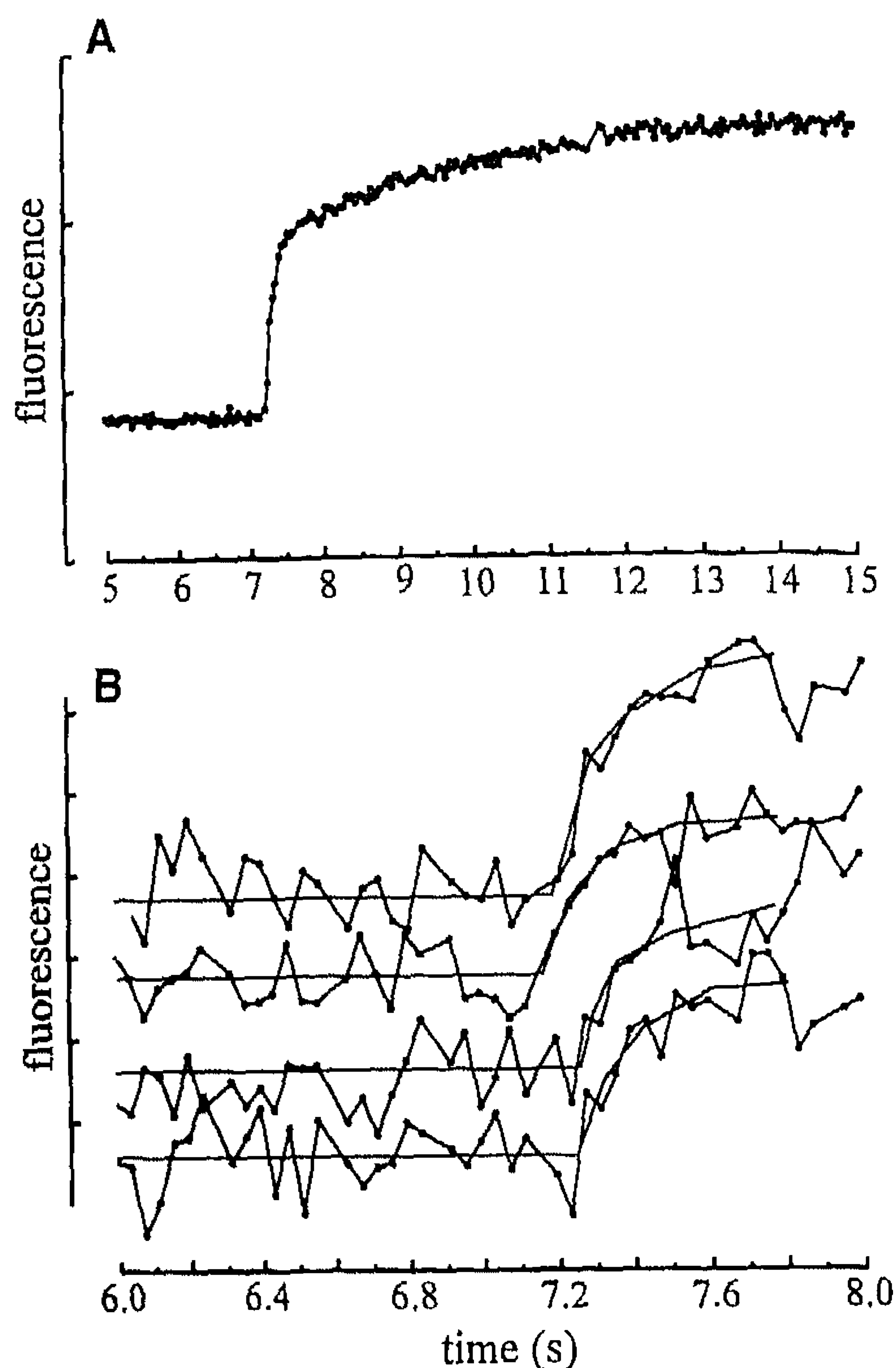


Fig. 3 Propagation of the Ca^{2+} spike throughout the monolayer. The onset of a spontaneous Ca^{2+} spike was recorded at 40 ms time intervals. (A) The average response of about 100 cells in the monolayer. Fluorescence intensity at 340 nm excitation is shown in arbitrary units. (B) The response of four groups of cells taken from (A) that were about 240 μm apart. In each group, the Ca^{2+} signal of three cells was averaged to reduce noise.

than 1000 cells simultaneously. Synchronous Ca^{2+} spikes could also be detected using this lower magnification, demonstrating that the Ca^{2+} spikes were synchronised throughout the entire monolayer (results not shown). Moreover, Ca^{2+} spikes were also seen using a conventional spectrofluorimeter in which the average signal of about 1 cm^2 of cells (approximately 1.0×10^5 cells) was recorded (results not shown). These spikes had the same shape and kinetics as the Ca^{2+} spikes recorded in single cells, which is only possible if the entire monolayer responded synchronously.

Although the virtually synchronous upstroke of the Ca^{2+} spikes in large numbers of cells indicated a mechanism other than a diffusion of a soluble second messenger, like Ca^{2+} or IP_3 , the time resolution of these dynamic video experiments was too low to rule out diffusion of a second messenger. Therefore, experiments were performed at a single wavelength (340 nm) at the highest possible time resolution in our system, i.e. 40 ms (video rate). Figure 3A, which depicts the average signal from close to 100 cells, shows the onset of a Ca^{2+} spike at

high time resolution. In less than 200 ms, the $[\text{Ca}^{2+}]_i$ reached almost its peak value. Figure 3B shows the same experiment at an expanded time scale with groups of cells that were separated from each other. To improve the signal to noise ratio, groups of 3 cells were taken and the four traces in Figure 3B represent the average Ca^{2+} signal in these groups. These four groups of cells in the monolayer were separated by about 8 cells. Thus, with an average cell diameter of 30 μm , these groups of cells were about 240 μm apart. Although there was considerable noise, due to the high sampling frequency, Figure 3B shows that the delay in the increase in $[\text{Ca}^{2+}]_i$ that could be detected was not more than 200 ms. The velocity of the signal underlying the virtually synchronous increase in $[\text{Ca}^{2+}]_i$ signal would be, therefore, at least 1000 $\mu\text{m}/\text{s}$. This is considerably higher than the fastest measured intracellular Ca^{2+} wave (160 $\mu\text{m}/\text{s}$; [21]) and rules out the possibility of a diffusible second messenger that triggers the Ca^{2+} spikes, but instead suggests an electrical signal.

External Ca^{2+} dependence of the spontaneous Ca^{2+} spikes

To investigate whether the synchronised Ca^{2+} spikes were caused by release of Ca^{2+} from intracellular stores or by the influx of Ca^{2+} from the extracellular medium, the effect of lowering the extracellular Ca^{2+} concentration on the occurrence of the Ca^{2+} spikes was studied. Figure 4A shows that the Ca^{2+} spikes were quickly abolished after perfusion of Ca^{2+} -free medium. Also, the baseline $[\text{Ca}^{2+}]_i$ decreased. Bradykinin (BK), which is known to release Ca^{2+} from intracellular stores, was still able to increase $[\text{Ca}^{2+}]_i$ under these Ca^{2+} -free conditions, demonstrating that intracellular Ca^{2+} stores were still filled. These results show that the increase in $[\text{Ca}^{2+}]_i$ was caused by the influx of Ca^{2+} from the extracellular medium. Ca^{2+} spikes were also abolished by the L-type Ca^{2+} channel blocker felodipine (1.0 μM ; Fig. 4B; [22]), indicating that Ca^{2+} entered the cell via L-type voltage-dependent Ca^{2+} channels. Neither Ca^{2+} -free media nor felodipine affected cell coupling via gap junctions (not shown) as measured by capacitance measurements [17].

The involvement of a voltage-sensitive Ca^{2+} channel again supports the role of membrane potential in Ca^{2+} spiking of the cells. We tried to evoke Ca^{2+} spikes with the L-type Ca^{2+} channel opener BAY K8644 [23] in density-arrested NRK monolayers that did not show spontaneous spikes, but results were not consistent. In some cases, Ca^{2+} spikes could be evoked with 1.0 μM BAY K8644, but in most cases BAY K8644 had no effect (data not shown). The involvement of voltage-dependent Na^+ channels was excluded by the fact that the potent voltage-dependent Na^+ channel blocker tetrodotoxin (TTX; [4]) did not affect the Ca^{2+} spikes (Fig. 4C).

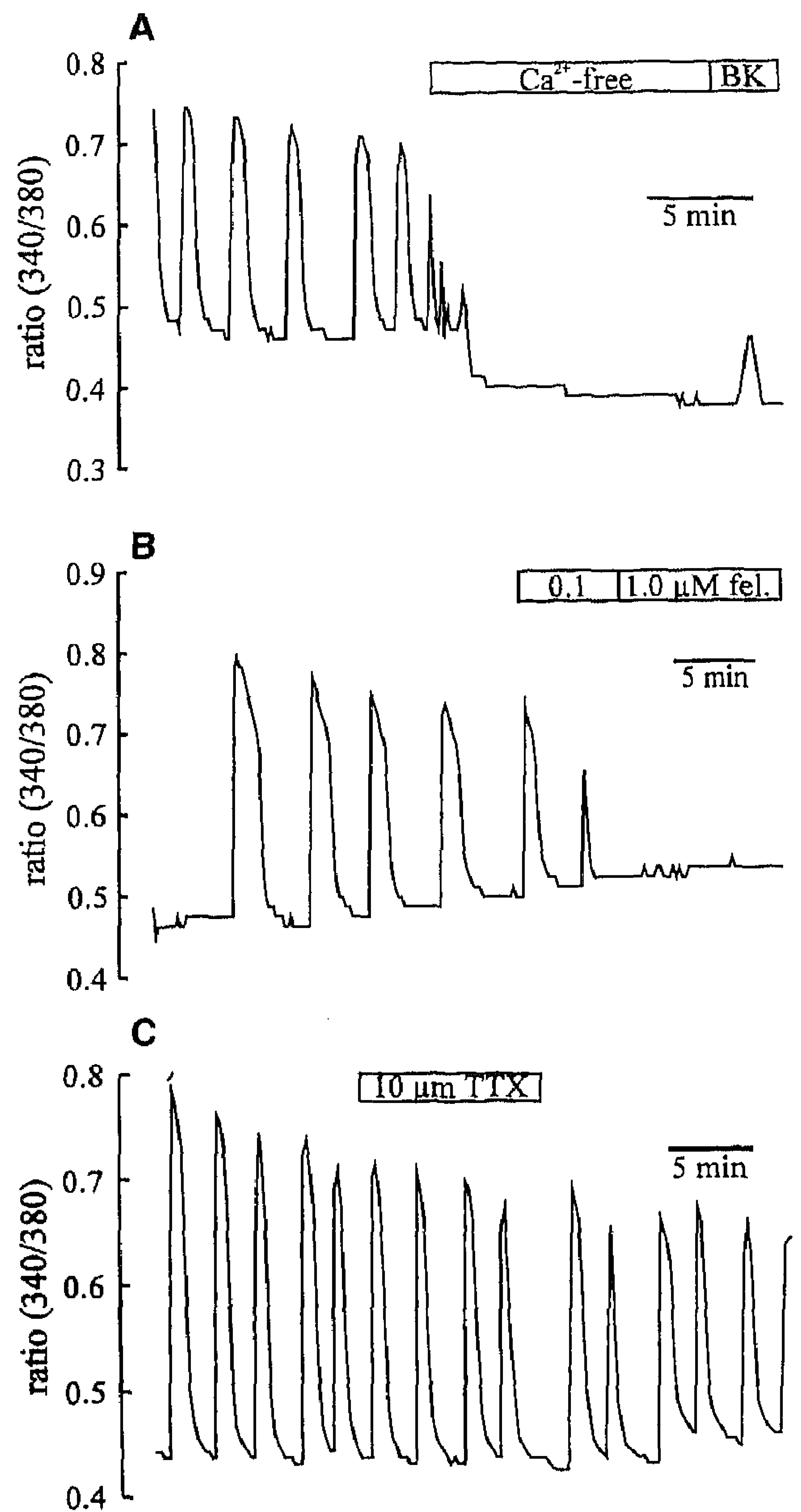


Fig. 4 Effect of extracellular Ca^{2+} , Ca^{2+} channel blockers and TTX on the Ca^{2+} spikes. Cells that exhibited spontaneous Ca^{2+} spikes were perfused with (A) Ca^{2+} -free medium supplemented with 1 mM EGTA, followed by 10 nM bradykinin (BK) in the same Ca^{2+} -free medium. (B) Cells were perfused with 0.1 and 1.0 μM felodipine, as indicated by the bars; and (C) cells were perfused with 10 μM tetrodotoxin (TTX). The bars above the experiments reflect the entering of the new perfusion medium to the bath and complete mixing required at least 30 s. Traces represent the average signal of about 100 cells. Traces of individual cells showed that all Ca^{2+} spikes were synchronised (not shown). Each trace is representative of at least three similar experiments

Block of the Ca^{2+} spikes by bradykinin and octanol

Propagation of an electrical signal through the monolayer requires electrical coupling of the cells through gap junctions. NRK cells are electrically well coupled via gap junctions [17,24]. Octanol, a strong inhibitor of gap

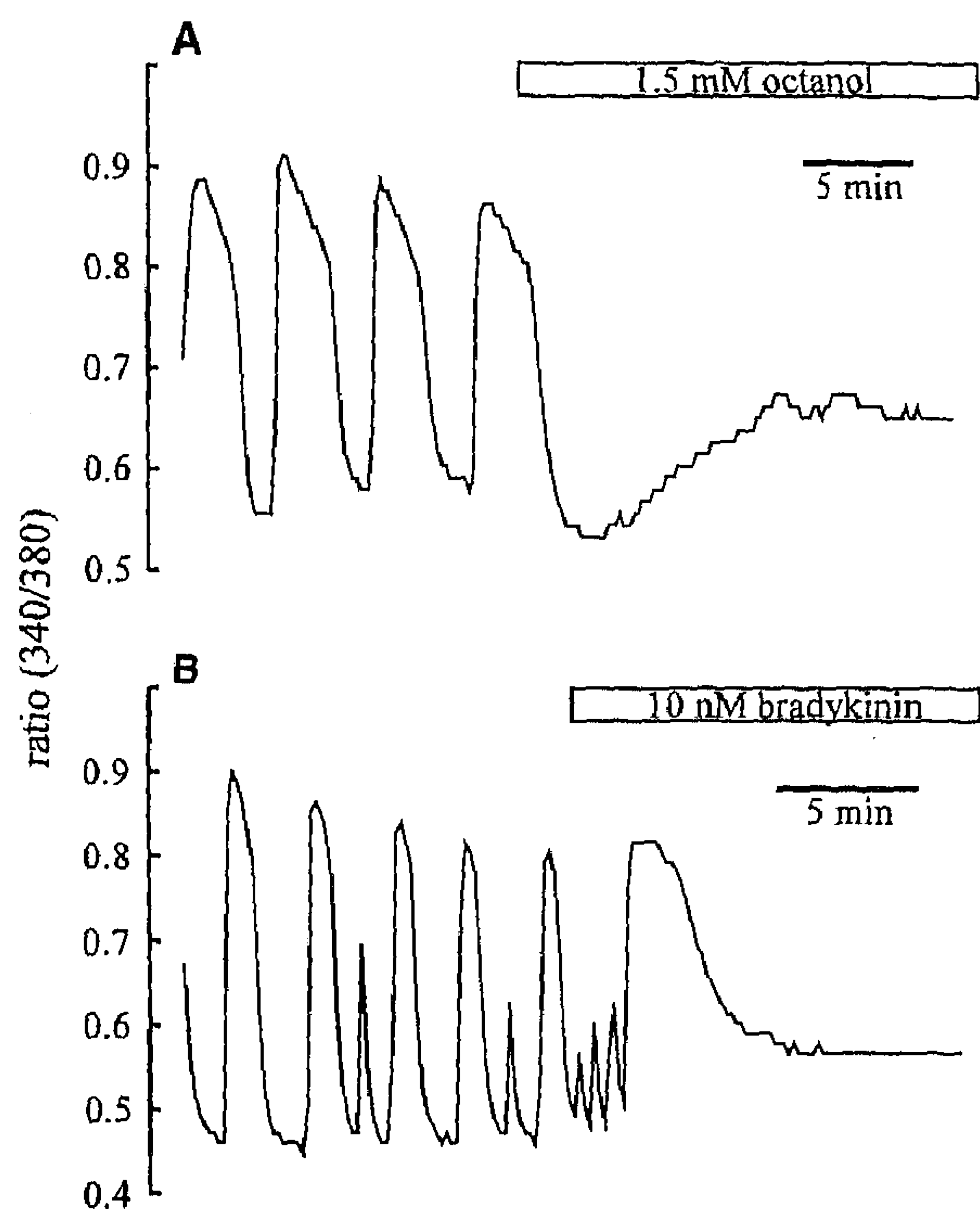


Fig. 5 The effect of octanol and bradykinin on the Ca^{2+} spikes. Cells were perfused with (A) 1.5 mM octanol and (B) 10 nM bradykinin (BK) during indicated times. Traces represent the average signal of about 100 cells.

junctional coupling in NRK cells [17], did not desynchronise the Ca^{2+} spikes, but blocked the synchronous spikes completely (Fig. 5A). This result indicates that gap junction-mediated intercellular communication plays an important role in spontaneous Ca^{2+} spiking of the density-arrested cells, although an aspecific effect of octanol on other membrane proteins such as ion channels cannot be excluded. Figure 5B shows that 10 nM bradykinin, which causes a long-lasting depolarisation (up to 15 min; [25]), also blocked the repetitive Ca^{2+} spikes. In addition, spikes were blocked by depolarisation of the cells with 60 mM K^+ (results not shown). The latter treatment evoked a single, transient rise in $[\text{Ca}^{2+}]_i$ (see also Fig. 10C), after which no spontaneous Ca^{2+} spikes were observed anymore. Neither BK nor depolarisation with K^+ affected cell coupling (data not shown). This block of repetitive Ca^{2+} spikes by a sustained depolarisation suggests that changes in membrane potential are necessary for the Ca^{2+} spikes to occur.

Spontaneous Ca^{2+} spikes are paralleled by membrane depolarisations

The virtually synchronised Ca^{2+} spiking of large numbers of cells, the involvement of voltage-dependent Ca^{2+} channels, the apparent requirement of electrical coupling

via gap junctions, and the block of spikes by a sustained depolarisation, all suggested a role of membrane depolarisations in the induction of Ca^{2+} spikes. By coloaded the cells with the fluorescent probe $\text{DiBAC}_4(3)$ and Fura-2, we were able to measure intracellular Ca^{2+} simultaneously with the membrane potential. Figure 6 shows that each synchronous Ca^{2+} spike (Fig. 6A) was paralleled by a depolarisation of the membrane (Fig. 6B). This is in agreement with the idea that an electrical signal underlies the Ca^{2+} spikes. Since $\text{DiBAC}_4(3)$ is a slow probe, membrane potential changes are followed by a relatively slow redistribution of the probe between cell and medium and, therefore, this experiment itself can not give information whether the membrane depolarisation preceded the Ca^{2+} spike or vice versa.

Patch clamp measurements of spontaneous membrane potential spikes

To further substantiate the role of membrane potential in the Ca^{2+} spikes, membrane potential was measured in the

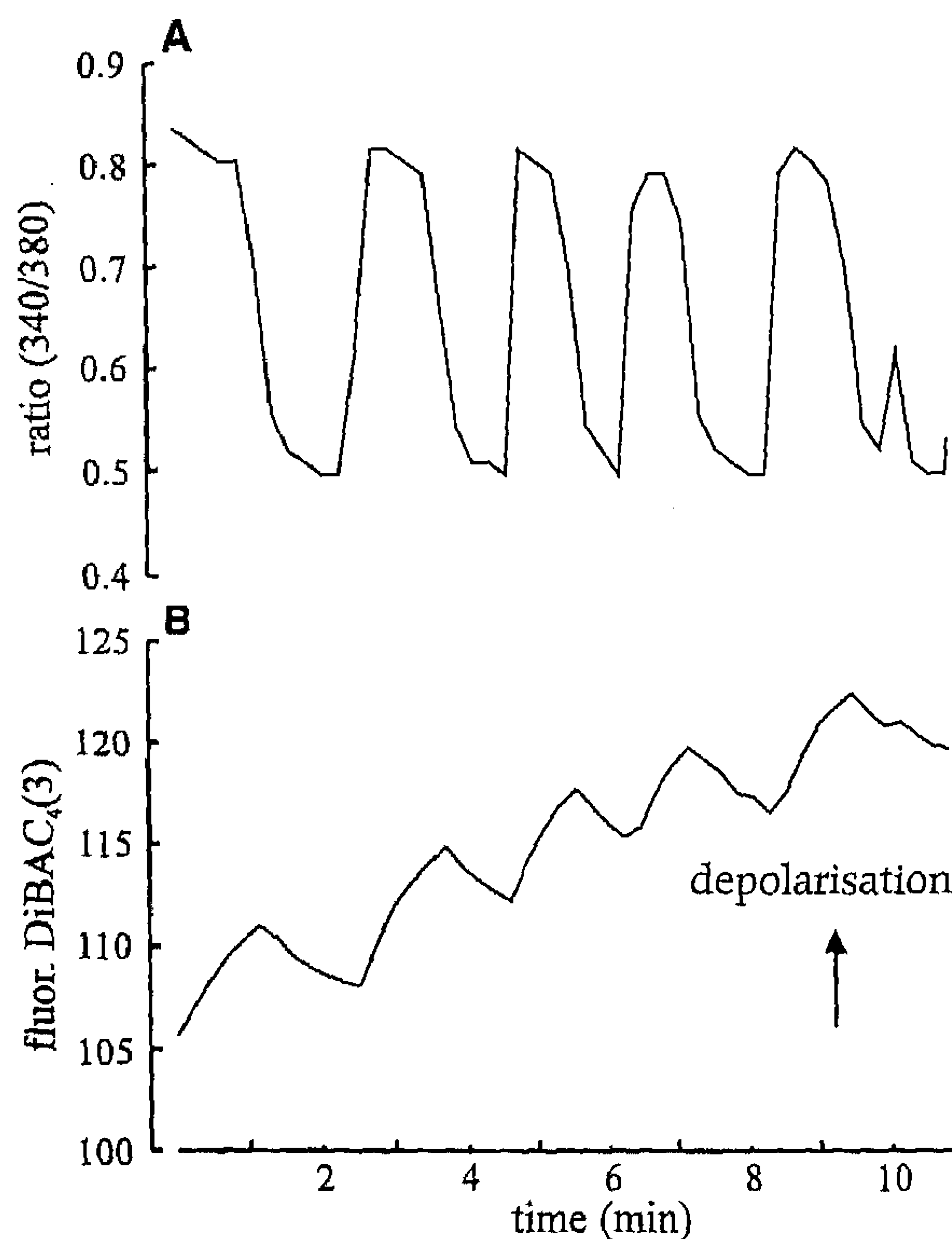


Fig. 6 Simultaneous measurements of intracellular Ca^{2+} and membrane potential. (A) Repetitive increases in $[\text{Ca}^{2+}]_i$ as measured by Fura-2 fluorescence. (B) Measurement of membrane potential using the fluorescent probe bisoxonol during the Ca^{2+} spikes shown in (A). Cells were loaded with Fura-2 as described in Materials and methods, 75 nM $\text{DiBAC}_4(3)$ was continuously present during the experiment. $\text{DiBAC}_4(3)$ fluorescence is shown in arbitrary units. The baseline shift of the $\text{DiBAC}_4(3)$ signal indicates an accumulation of the probe in the cell during the experiment. Excitation wavelengths for Fura-2 and $\text{DiBAC}_4(3)$ were alternately used to monitor both $[\text{Ca}^{2+}]_i$ and membrane potential.

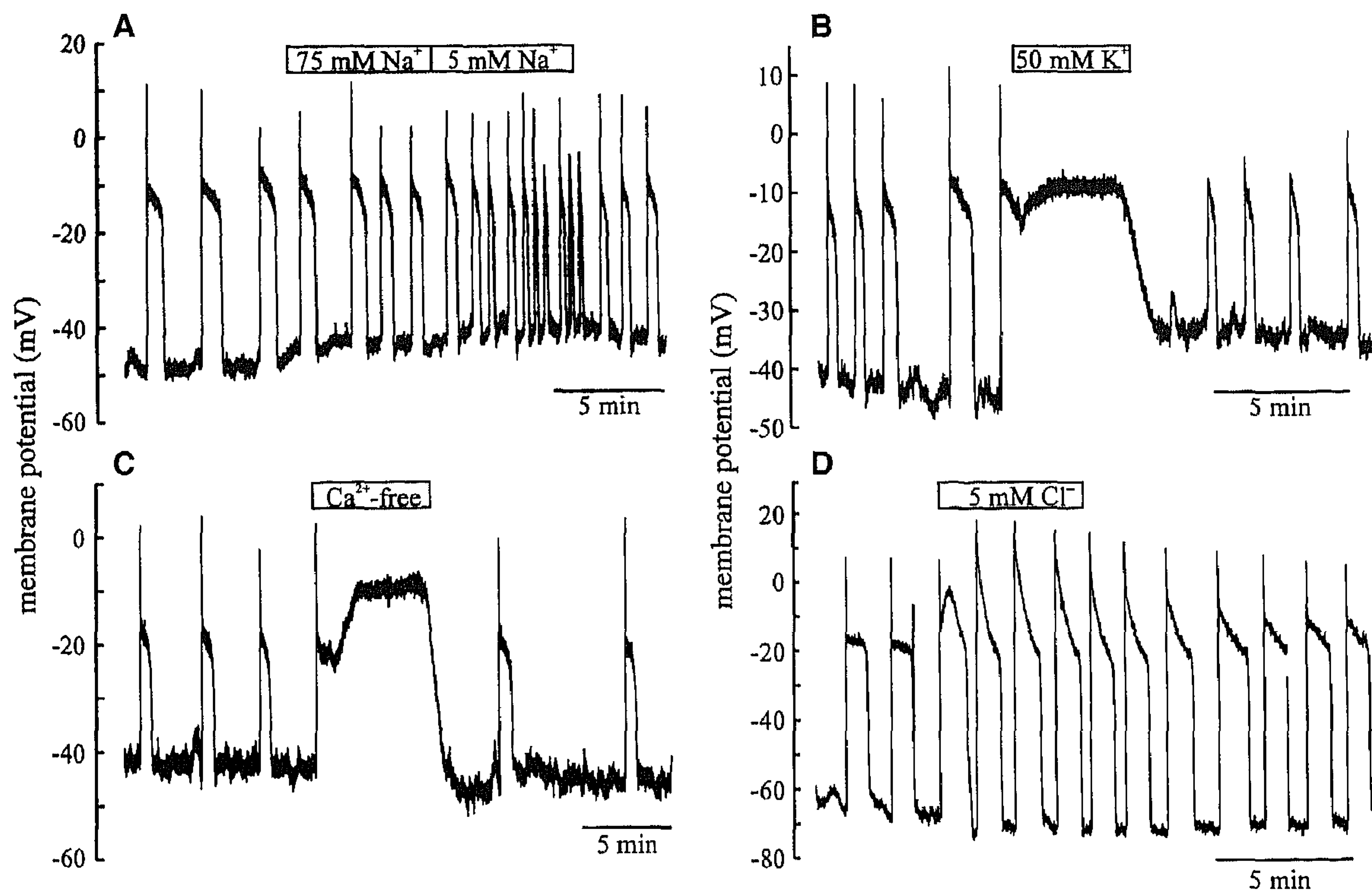


Fig. 7 Patch clamp measurements of repetitive membrane potential spikes. Ion substitutions were performed in order to determine ionic dependence of the spikes. (A) Cells were perfused with medium containing 75 mM and 5 mM Na^+ during indicated times. (B) Cells were depolarised by perfusion of medium containing 50 mM K^+ . (C) Perfusion with Ca^{2+} -free medium supplemented with 1 mM EGTA. (D) Perfusion with medium containing 5 mM Cl^- . Membrane potential was recorded in the current clamp mode of the whole cell patch clamp technique. Shown are typical experiments that were repeated at least four times with similar results.

current clamp mode of the patch clamp technique. Since monolayers of NRK cells are electrically well coupled, always an average membrane potential will be measured when a single cell in the monolayer is patched. Using this configuration of the patch-clamp technique, spontaneous spike-like depolarisations ('membrane potential spikes') were regularly observed in density-arrested monolayers of NRK fibroblasts (Fig. 7A–D). These membrane potential spikes had a similar frequency and shape as the Ca^{2+} spikes. The membrane depolarised usually within 100 ms in an all-or-none, action potential-like manner from a resting potential between -60 and -40 mV to a peak value that could be as high as $+20$ mV and which lasted only a few milliseconds. After this fast depolarisation, the membrane quickly repolarised to a plateau value at around -10 mV, during which the membrane only slowly repolarised to a threshold value of around -20 mV. Subsequently, membrane potential quickly returned to its resting value.

In patch clamp experiments, the incidence of spontaneous spikes in physiological DF media with a normal pH of 7.4 was about 50% and, therefore, media with a pH of 7.4 were used in the patch clamp measurements.

Medium with a high pH increased the duration of the plateau phase of the membrane potential spikes similar to the Ca^{2+} spikes (results not shown). Of note, in the patch clamp experiments, spontaneous membrane potential spikes were seen only in density-arrested cells, and never in quiescent NRK cells.

Ionic basis of the membrane potential spikes

Ion substitution experiments were performed to study the ionic basis of the membrane potential spikes. Figure 7A shows the membrane potential spikes in medium in which the Na^+ concentration was successively lowered to 75 and 5 mM. The magnitude of the spikes and the onset of the rapid decay phase was not changed by low Na^+ -media, only the frequency of the spikes increased in 5 mM Na^+ , whereas the duration of the plateau phase was decreased. Of note, changes in frequency were sometimes also seen spontaneously. Since TTX did not affect the frequency of the Ca^{2+} spikes, the increased frequency in low Na^+ media may, therefore, not be related to a Na^+ conductance, but instead be caused by the abnormal ion constitution in low Na^+ media.

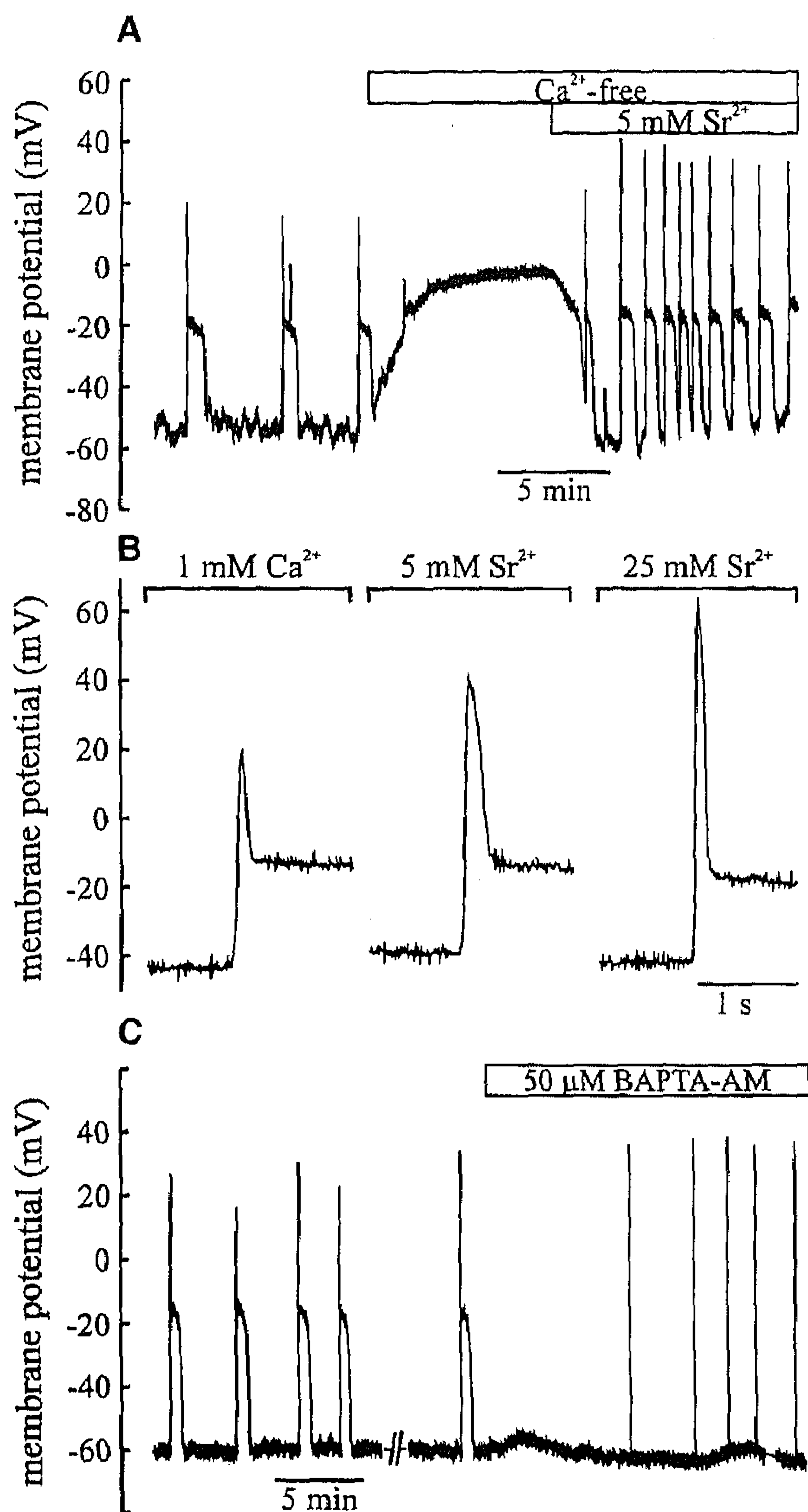


Fig. 8 Effect of Sr²⁺ on the membrane potential spikes and the role of intracellular Ca²⁺. (A) Spontaneously spiking monolayers were first perfused with a Ca²⁺-free medium (1 mM EGTA) to abolish the spikes, after which 5 mM Sr²⁺ was added to this medium. (B) Magnitude of the peak depolarisation in 1 mM Ca²⁺, and in medium supplemented with 5 and 10 mM Sr²⁺, respectively. Shown are representative traces of at least three experiments. (C) Spontaneously spiking cells were perfused with 50 μM BAPTA/AM to buffer intracellular Ca²⁺. Interruption of the trace represents a 5 min gap in which voltage-clamp experiments were performed. One spike occurred in this period.

Depolarisation of the cells by 50 mM K⁺ (Fig. 7B) reversibly abolished the membrane potential spikes completely. Also, perfusion of Ca²⁺-free media (3 mM EGTA) reversibly blocked the spikes (Fig. 7C). Ca²⁺-free media with low concentrations of EGTA (1.0 mM and less) sometimes induced fast dampened membrane potential oscillations (not shown). Ca²⁺-free media also

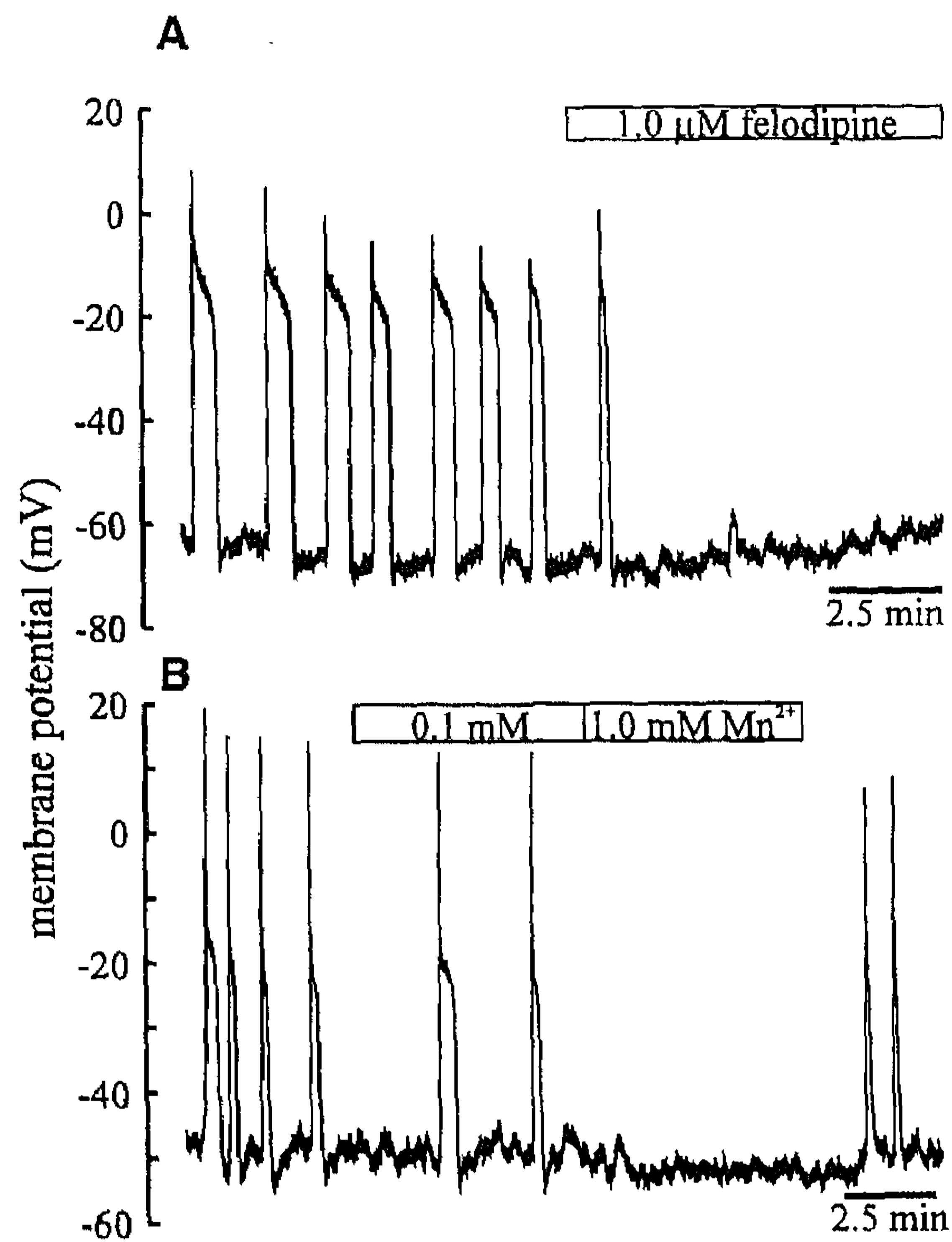


Fig. 9 Effect of felodipine and Mn²⁺ on the membrane potential spikes. Spontaneously spiking monolayers were perfused with (A) 1.0 μM felodipine and (B) 0.1 and 1.0 mM Mn²⁺.

depolarised the cells to a sustained level of -10 mV, a process that was quickly reversed upon re-addition of Ca²⁺. This depolarisation may be explained by the phenomenon that Ca²⁺ channels may become permeable to Na⁺ [4] at very low concentrations of Ca²⁺, or by the opening of non-specific cation channels by the removal of Ca²⁺ from the extracellular medium [26].

Figure 7D shows that a low Cl⁻ medium only slightly increased the magnitude of the initial fast part of the depolarisation, but changed the plateau phase significantly. In 5 mM Cl⁻, the membrane repolarised slowly from the peak of the spike, instead of the initial fast repolarisation to -10 mV observed in control medium. Although the plateau phase was affected by low Cl⁻ media, the membrane potential at which the membrane started to repolarise quickly (-20 mV), was not affected. These results show that the magnitude of the fast peak depolarisation is hardly influenced by Na⁺ and Cl⁻ and that these ions are not responsible for the initial depolarisation.

The role of extra- and intracellular Ca²⁺ in the membrane potential spikes

Depolarisations that overshoot 0 mV can be carried by Na⁺ or Ca²⁺ since the Nernst equilibrium potentials for both ions are positive. However, changing the Na⁺ concentration

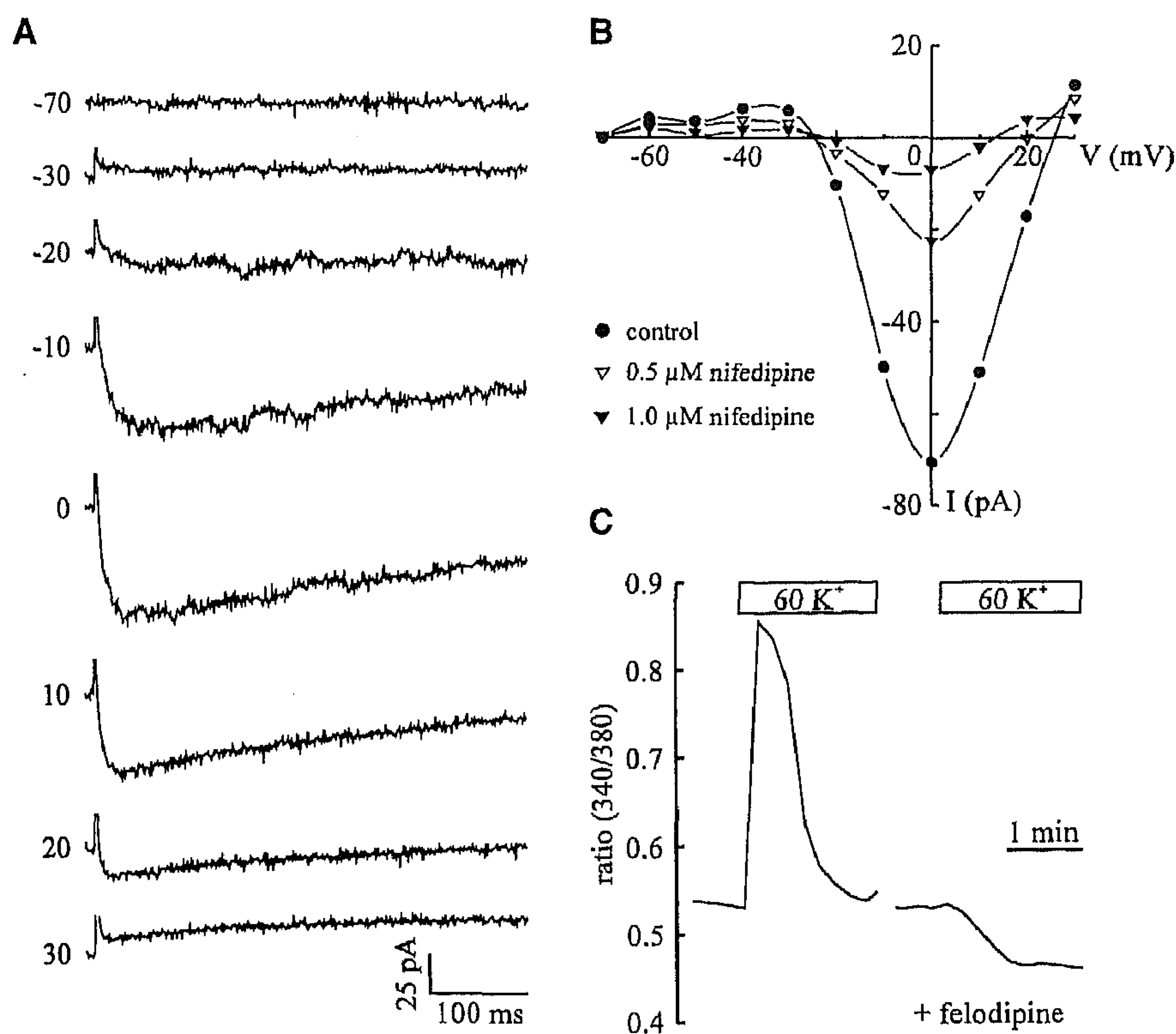


Fig. 10 Voltage-dependent Ca^{2+} currents. **(A)** Whole cell inward currents elicited by 10 mV depolarising steps from a holding potential of -70 mV, using Ba^{2+} as the charge carrier. **(B)** Current voltage relation of the peak Ba^{2+} currents shown above and the effect 0.5 and 1.0 μM of the L-type Ca^{2+} channel blocker nifedipine. **(C)** The effect of depolarisation of monolayers of NRK cells by perfusing 60 mM K^{+} in the absence and presence of 1.0 μM felodipine.

did not affect the magnitude of the depolarisation (Fig. 7A). Since Ca^{2+} -free media abolished the membrane potential spikes, it was investigated whether an increased Ca^{2+} permeability was responsible for the initial depolarisation. Since Sr^{2+} can readily permeate Ca^{2+} channels [4], Sr^{2+} was substituted for Ca^{2+} . Figure 8A shows that, after a block of the membrane potential spikes with Ca^{2+} -free medium (supplemented with 1 mM EGTA), 5 mM Sr^{2+} could re-establish membrane potential spikes. Also, the magnitude of the initial depolarisation was higher in 5 mM Sr^{2+} than in 1 mM Ca^{2+} . If the depolarising spike is caused by an increased Ca^{2+} permeability, it is to be expected that increasing the concentration gradient for Ca^{2+} , or Sr^{2+} in this case, will increase the magnitude of the membrane potential spike. Figure 8B shows the first part of the membrane potential spike in media with 1 mM Ca^{2+} , 5 mM Sr^{2+} and 25 mM Sr^{2+} , respectively, and demonstrates that increasing the concentration of Sr^{2+} in the medium indeed increased the magnitude of the initial depolarising spike, without affecting the plateau phase. In control solutions with 1 mM Ca^{2+} , the depolarisation reached $+20$ mV, while in 5 and 25 mM Sr^{2+} the initial depolarisation was markedly increased to $+40$ mV and $+60$ mV, respectively. This corresponds with a 29 mV increase in spike depolarisation

per 10-fold increase in concentration, which is in good agreement with the expected value for permeation of divalent ions [4]. These results clearly show that the depolarising membrane potential spike is caused by an increased Ca^{2+} permeability.

The role of intracellular $[\text{Ca}^{2+}]_i$ in the membrane potential spikes was investigated by loading the cells with the Ca^{2+} chelator BAPTA. The acetoxymethyl ester of BAPTA was perfused to cells that showed repetitive membrane potential spikes (Fig. 8C). Loading the cells with BAPTA blocked the plateau phase of the spike, while leaving the initial depolarising spike intact. As a result, the membrane potential spikes consisted of the normal fast depolarisation, followed by an immediate complete repolarisation. The magnitude of the depolarisation was also slightly increased, which can be explained by an increased concentration gradient for Ca^{2+} when intracellular Ca^{2+} is buffered. These results show that the initial spike is not dependent on the $[\text{Ca}^{2+}]_i$, as expected when the influx of Ca^{2+} from the extracellular medium through Ca^{2+} channels is responsible for this depolarisation. In addition, these results show convincingly that intercellular transfer of Ca^{2+} is not necessary for the occurrence of the calcium and membrane potential spikes

(see Fig. 2). On the other hand, the plateau phase of the membrane potential spike clearly depends on $[Ca^{2+}]_i$.

The role of L-type Ca^{2+} channels in the membrane potential spikes

The block of the Ca^{2+} spikes by felodipine (Fig. 4B) suggested the involvement of L-type Ca^{2+} channels in the repetitive spiking of the membrane potential. Figure 9A shows that 1.0 μ M felodipine blocked the membrane potential spikes as well, an effect that was also exerted by 1.0 μ M nifedipine (not shown) and 1.0 mM Mn^{2+} (Fig. 9B), two other blockers of L-type Ca^{2+} channels [23,27].

To further support the presence of voltage-dependent Ca^{2+} channels in NRK cells, Ca^{2+} currents were evoked in single, trypsinised NRK cells, using Ba^{2+} as the charge carrier. In the whole cell voltage clamp configuration, cells were stepwise depolarised from a holding potential of -70 mV. Figure 10A shows typical recordings of the resulting inward current traces. Ba^{2+} currents could be consistently evoked after depolarisation beyond a threshold of around -20 mV with a peak current at 0 mV (Fig. 10B). Nifedipine (Fig. 10B) and felodipine (not shown) blocked the Ba^{2+} currents dose-dependently. These results are consistent with the presence of L-type Ca^{2+} channels in NRK fibroblasts. In monolayers that showed no spontaneous Ca^{2+} spikes, depolarisation of monolayers of NRK cells with high extracellular K^+ evoked an increase in $[Ca^{2+}]_i$ (Fig. 10C), which reflects the opening of voltage-dependent Ca^{2+} channels under physiological culture conditions. Despite the prolonged depolarisation with K^+ , $[Ca^{2+}]_i$ returned to its basal value. Felodipine prevented this increase in $[Ca^{2+}]_i$ completely and, for unknown reasons, even reduced $[Ca^{2+}]_i$ upon depolarisation. These results confirmed the presence of voltage-dependent, L-type Ca^{2+} channels in NRK fibroblasts.

DISCUSSION

Synchronised Ca^{2+} spiking of density-arrested NRK cells

The results presented here show that monolayers of density-arrested NRK fibroblasts exhibit spontaneous Ca^{2+} spikes that are synchronised throughout the monolayer. Synchronised Ca^{2+} oscillations have also been shown in monolayers of endothelial cells [28–30], in electrically active pancreatic β -cells [7,31] and in human sweat gland epithelial cells [32]. In most cases, the underlying mechanism was unknown. In other cell types, intercellularly propagating Ca^{2+} waves have been reported [30,33,34] that probably result from the regenerative production of IP_3 by the diffusion of Ca^{2+} and/or IP_3 through gap junctions to neighbouring cells with concomitant Ca^{2+} release from intracellular stores [2].

Ca^{2+} action potentials underlie synchronous Ca^{2+} spiking

The signal that is responsible for the synchronisation of the Ca^{2+} rise in the monolayer was at least 1000 μ m/s and too fast to be explained by the diffusion of a second messenger like Ca^{2+} or IP_3 . The fastest velocity of an intracellular Ca^{2+} wave has been reported to occur in heart myocytes and was 160 μ m/s [21], while the velocity of intercellular Ca^{2+} waves is in the range of 2–20 μ m/s [35].

We also show here that the synchronised Ca^{2+} spikes in NRK cells are not the result of diffusion of Ca^{2+} between cells, but instead of an influx of Ca^{2+} from the extracellular medium. Taken together, it is unlikely that the repetitive Ca^{2+} spikes observed in the present study can be explained by intercellular diffusion of second messengers or a periodic release of Ca^{2+} from intracellular stores as has been proposed in other cell types [2,23,36]. Instead, this high degree of synchronisation suggests a rapidly propagating, regenerative electrical signal, i.e. an action potential.

Ca^{2+} spikes were paralleled by membrane potential depolarisations as shown by the bisoxonol measurements (Fig. 6). However, whether the membrane depolarisations preceded the Ca^{2+} spikes could not be resolved using this slow membrane potential probe. Current clamp patch clamp measurements revealed that these depolarisations were in fact membrane potential spikes displaying the same shape and frequency as the Ca^{2+} spikes. The membrane potential spikes were fast, occurred in an all-or-none fashion and resembled action potentials.

From the synchronicity of the Ca^{2+} spikes, it is concluded that rapidly propagating membrane potential spikes must underlie the Ca^{2+} spikes. Since monolayers of NRK cells are electrically well coupled via gap junctions [17], this provides a way for the fast transduction of changes in membrane potential.

The membrane potential spikes in NRK cells met all criteria for a Ca^{2+} action potential [5]: Ca^{2+} action potentials are characterised by an overshoot that increases with increasing concentrations of extracellular Ca^{2+} (Sr^{2+}), they continue in Na^+ -free media, and can be blocked by Ca^{2+} channel antagonists. In that respect, Ca^{2+} action potentials and associated Ca^{2+} spikes resemble those that are present in virtually all excitable cells, ranging from invertebrate muscle to various vertebrate muscle, endocrine cells, and granulosa cells [5,37–39].

The involvement of L-type Ca^{2+} channels in the upstroke of the Ca^{2+} action potential

The inhibition of both the Ca^{2+} and membrane potential spikes by L-type voltage-dependent Ca^{2+} channel blockers indicates that these channels mediate the Ca^{2+} action potential. It has been reported before that

fibroblasts can possess L-type Ca^{2+} channels [8,9,11,12], but a function for such channels in these cells has so far been unclear. Here, we show that NRK fibroblasts also possess L-type voltage-dependent Ca^{2+} channels (Fig. 10). As the activity of L-type Ca^{2+} channels has been shown to be higher at more alkaline pH [40], this may explain why the incidence of spontaneous repetitive Ca^{2+} spikes was increased in alkaline media.

The plateau and repolarisation phase of the Ca^{2+} action potential

The plateau phase of the Ca^{2+} action potential was determined by an increased chloride conductance and was abolished by buffering the rise in $[\text{Ca}^{2+}]_i$. This indicates the involvement of a Ca^{2+} -activated chloride conductance. Recently, we showed that BK depolarises NRK cells to -15 mV by a Ca^{2+} -activated chloride conductance [25], which is in agreement with the results obtained here. Thus, the influx of Ca^{2+} , concomitant with every Ca^{2+} action potential, activates a Ca^{2+} -dependent chloride conductance, which prolongs the action potential. Substitution of Ca^{2+} by Sr^{2+} also evoked a plateau phase, indicating that the influx of Sr^{2+} is sufficient to cause activation of the Ca^{2+} -activated Cl^- channels.

During the plateau phase of the action potential, the intracellular Ca^{2+} level only slowly declined. At this increased Ca^{2+} level, it is expected that Ca^{2+} -ATPases are fully active [4]. The fast decline in intracellular Ca^{2+} after the plateau phase shows that the Ca^{2+} -ATPases have a sufficient capacity to pump the Ca^{2+} out of the cytosol. Therefore, the increased Ca^{2+} level during the plateau phase implies a continuous flux of Ca^{2+} into the cytosol. Mn^{2+} quenching experiments [41] suggested a Ca^{2+} influx from the extracellular medium during the entire depolarisation (de Roos et al., unpublished). A possible source may be an influx of Ca^{2+} through L-type Ca^{2+} channels, since these channels have a slow inactivation rate [23], and small L-type Ca^{2+} currents can persist for several minutes [42,43]. The slow decrease to basal $[\text{Ca}^{2+}]_i$ levels after an initial increase by a continuous depolarisation (Fig. 10C) may reflect this slow inactivation. However, it remains to be established whether other sources, such as Ca^{2+} -induced Ca^{2+} release [36], might be responsible for the rise in $[\text{Ca}^{2+}]_i$.

Whereas the slow repolarisation during the plateau phase may be caused by a decreasing activity of Ca^{2+} -activated Cl^- channels, the onset of further repolarisation to resting values was not affected by the extracellular Cl^- , but always occurred at a membrane potential of around -20 mV, suggesting a threshold for repolarisation. Although the decrease in $[\text{Ca}^{2+}]_i$ also showed synchronisation, the fact that prolonged depolarisation with high

extracellular K^+ caused only a transient increase in $[\text{Ca}^{2+}]_i$ (Fig. 10C), argues against a membrane potential-regulated decrease of $[\text{Ca}^{2+}]_i$ levels. Therefore, the mechanism underlying the fast repolarisation is unknown, but might be caused by a re-opening of inward rectifying K^+ channels that closed during the action potential as shown for cardiac action potentials [4].

Induction and propagation of the Ca^{2+} action potential

A general characteristic of action potentials is that they can be induced by a depolarisation beyond a threshold value. The maximum current that could be injected with our patch clamp set-up (500 pA) only changed the membrane potential by 3–5 mV and, therefore, voltage clamp experiments could not be used to evoke action potentials. Since the membrane potential of density-arrested NRK fibroblasts is -40 to -60 mV, and the L-type Ca^{2+} channels that are involved in the depolarisation have a threshold for activation between -30 mV and -10 mV [4,23], activation of the L-type channels, requires an initial depolarisation of the membrane to this threshold. Although, in most cases, no slow increase to a threshold value could be detected before the onset of the depolarising membrane potential spike, gradual depolarisations preceding the action potential-like depolarisation were observed occasionally. It is proposed that the initiation of the spikes occurs randomly in the monolayer, in which case a part of the monolayer slowly depolarises to the threshold value of L-type Ca^{2+} channels, after which a propagating action potential evolves.

We showed recently that depolarisation beyond the threshold for L-type Ca^{2+} channels upon addition of a high concentration of extracellular K^+ could induce a propagating action potential in monolayers of quiescent NRK fibroblasts which do not show spontaneous spikes (de Roos et al., submitted). These action potentials had a propagation velocity of 6.0 mm/s, which is in agreement with the minimal velocity of 1.0 mm/s that could be assessed in the present study and suggests that the Ca^{2+} spikes reported here are evoked by Ca^{2+} action potentials that originated somewhere in the monolayer and subsequently propagated through the monolayer.

Since monolayers of NRK cells are electrically well coupled and the membrane potential will be an average of many cells, it is expected that the behaviour of ion channels in a single cell will not be sufficient to change the membrane potential beyond the threshold value for L-type Ca^{2+} channels due to electrotonic spread to neighbouring cells. Furthermore, the fact that single cells (in isolation) do not show spontaneous action potentials (de Roos et al., unpublished), does not support a role for random behaviour of single cells as a possible trigger for the generation of the action potential.

Model for Ca²⁺ and membrane potential spikes

The following model is proposed. Randomly in the monolayer, a spontaneous depolarising trigger, whose nature is so far unknown, opens voltage-dependent L-type Ca²⁺ channels. Opening of Ca²⁺ channels generates an influx of Ca²⁺ in the cells with a concomitant further depolarisation towards the equilibrium potential for Ca²⁺. Transduction of this depolarisation to neighbouring cells via gap junctions causes the regenerative opening of Ca²⁺ channels in these cells, resulting in active propagation of the signal through the whole monolayer. The influx of Ca²⁺ during the action potential opens a Ca²⁺-activated Cl⁻ conductance, responsible for the plateau phase of the action potential. A decreased [Ca²⁺]_i inactivates Cl⁻ channels, ultimately resulting in repolarisation by a so far unknown mechanism.

Ca²⁺ signaling in fibroblasts

Since fibroblast(-like) cells can be electrically coupled to each other [13,15–17]) and may even form three-dimensional communicating networks in vivo [14,16], it is hypothesised that Ca²⁺ action potentials play a role in the co-ordination of Ca²⁺ signals in fibroblasts.

We show that the depolarisations associated with Ca²⁺ action potentials provide a novel mechanism for [Ca²⁺]_i signaling in fibroblasts that were hitherto considered to be inexcitable cells. Ca²⁺ action potentials provide fibroblasts with a mechanism for fast, all-or-none Ca²⁺ responses, similar to excitable cells. In classical models, an initial Ca²⁺ release from intracellular stores is amplified by an additional influx of Ca²⁺ via Ca²⁺ channels (I_{CRAC}) in the membrane [1,44] or a Ca²⁺-induced Ca²⁺ release mechanism [36]. The role of a release of Ca²⁺ from intracellular stores during the Ca²⁺ action potential remains to be established.

Density-dependent growth inhibition or density-arrest is characteristic of many non-transformed cells in culture and it is lost upon cellular transformation [18]. The elucidation of the largely unknown mechanisms that underlie density-arrest may be important to the further understanding of cellular growth control and transformation. Remarkably, spontaneous repetitive Ca²⁺ action potentials were only seen in density-arrested cells and never in quiescent cells. This might reflect differences in the number or regulation of the channel(s) involved. The ability to generate spontaneous Ca²⁺ action potentials apparently depends on growth status and may be involved in acquiring density-arrest of cell proliferation. We are currently investigating a possible density-dependent modulation of L-type Ca²⁺ channels in NRK cells. Although Ca²⁺ action potentials could be induced in quiescent cells in physiological concentrations of Ca²⁺

in about 10% of the cases, consistent induction required substitution of Sr²⁺ for Ca²⁺ (de Roos et al., submitted). In this paper, we showed that Ca²⁺ action potentials are consistently present in density-arrested cells at physiological concentrations of Ca²⁺ and may, therefore, be physiologically relevant.

ACKNOWLEDGEMENT

This research was funded by The Netherlands Foundation for Life Sciences.

REFERENCES

1. Putney Jr JW. Excitement about calcium signaling in inexcitable cells. *Science* 1993; **262**: 676–678.
2. Sanderson MJ, Charles AC, Boitano S, Dirksen ER. Mechanisms and function of intercellular calcium signaling. *Mol Cell Endocrinol* 1994; **98**: 173–187.
3. McPherson PS, Campbell KP. The ryanodine receptor/Ca²⁺ release channel. *J Biol Chem* 1993; **268**: 13765–13768.
4. Hille B. *Ionic channels in excitable membranes*. Sunderland, MA: Sinauer, 1992.
5. Hagiwara S, Byerly L. Membrane biophysics of calcium currents. *Fed Proc* 1981; **40**: 2220–2225.
6. De Mello WC. Gap junctional communication in excitable tissues: the heart as paradigm. *Prog Biophys Mol Biol* 1994; **61**: 1–35.
7. Santos RM, Rosario LM, Nadal A, Garcia-Sancho J, Soria B, Valdeolmillos M. Widespread synchronous [Ca²⁺]_i oscillations due to bursting electrical activity in single pancreatic islets. *Pflügers Arch* 1991; **418**: 417–422.
8. Chen C, Corbley MJ, Roberts TM, Hess P. Voltage-sensitive calcium channels in normal and transformed 3T3 fibroblasts. *Science* 1988; **239**: 1024–1026.
9. Lovisollo D, Alloatti G, Bonelli G, Tessitori L, Baccino FM. Potassium and calcium currents and action potentials in mouse Balb/c 3T3 fibroblasts. *Pflügers Arch* 1988; **412**: 530–534.
10. Peres A, Sturani E, Zippel R. Properties of the voltage-dependent calcium channel of mouse Swiss 3T3 fibroblasts. *J Physiol* 1988; **401**: 639–655.
11. Baumgarten LB, Toscas K, Villereal ML. Dihydropyridine-sensitive L-type Ca²⁺ channels in human foreskin fibroblast cells. *J Biol Chem* 1992; **267**: 10542–10530.
12. Harootunian AT, Kao JPY, Paranjape S, Tsien RY. Generation of calcium oscillations in fibroblasts by positive feedback between calcium and IP₃. *Science* 1991; **251**: 75–77.
13. Salomon D, Saurat J-H, Meda P. Cell-to-cell communication within intact human skin. *J Clin Invest* 1988; **82**: 248–254.
14. Komuro T. Re-evaluation of fibroblasts and fibroblast-like cells. *Anat Embryol* 1990; **182**: 103–112.
15. Hashizume T, Imayama S, Hori Y. Scanning electron microscopic study on dendritic cells and fibroblasts in connective tissue. *J Electron Microscop* 1992; **41**: 434–437.
16. Jester JV, Petroll WM, Barry PA, Cavanagh HD. Temporal, 3-dimensional, cellular anatomy of corneal wound tissue. *J Anat* 1995; **186**: 301–311.
17. De Roos ADG, van Zoelen EJJ, Theuvenet APR. Determination of gap junctional intercellular communication by capacitance measurements. *Pflügers Arch* 1996; **431**: 556–563.
18. Van Zoelen EJJ. Density-dependent control of cell proliferation: molecular mechanisms involved in contact-inhibition. In:

- Paukovitz W.R. ed. *Growth Regulation and Carcinogenesis*, vol. 1. Boca Raton: CRC Press, 1991; 91–93.
19. Van Zoelen EJJ, Van Oostwaard TMJ, De Laat SW. The role of polypeptide growth factors in phenotypic transformation of normal rat kidney cells. *J Biol Chem* 1988; **263**: 64–68.
 20. Willems PHGM, Van Emst-De Vries SE, Van Os CH, De Pont JJHMM. Dose-dependent recruitment of pancreatic acinar cells during receptor-mediated calcium mobilization. *Cell Calcium* 1993; **14**: 145–159.
 21. Jaffe LF. The path of calcium in cytosolic calcium oscillations: a unifying hypothesis. *Proc Natl Acad Sci USA* 1991; **88**: 9883–9887.
 22. Walton T, Symes LR. Felodipine and isradipine: new calcium-channel-blocking agents for the treatment of hypertension. *Clin Pharm* 1993; **12**: 261–275.
 23. Tsien RW, Tsien RY. Calcium channels, stores, and oscillations. *Annu Rev Cell Biol* 1990; **6**: 715–760.
 24. Maldonado PE, Rose B, Loewenstein WR. Growth factors modulate junctional cell-to-cell communication. *J Membr Biol* 1988; **106**: 203–210.
 25. De Roos ADG, van Zoelen EJJ, Theuvenet APR. Membrane depolarization in NRK fibroblasts is mediated by a calcium-dependent chloride conductance. *J Cell Physiol* 1997; **170**: 166–173.
 26. Krattenmacher R, Voigt R, Heinz M, Clauss W. Electrolyte transport through a cation-selective ion channel in large intestinal enterocytes of *Xenopus laevis*. *J Exp Biol* 1991; **115**: 275–290.
 27. Hancox JC, Levi JL. L-type calcium current in rod- and spindle-shaped myocytes isolated from rabbit atrioventricular node. *Am J Physiol* 1994; **267**: H1670–H1680.
 28. Sage SO, Adams DJ, Van Breemen C. Synchronized oscillations in cytoplasmic free calcium concentration in confluent bradykinin-stimulated bovine pulmonary artery endothelial cell monolayers. *J Biol Chem* 1989; **264**: 6–9.
 29. Neylon CB, Irvine RF. Synchronized repetitive spikes in cytoplasmic calcium in confluent monolayers of human umbilical vein endothelial cells. *FEBS Lett* 1990; **275**: 173–176.
 30. Laskey RE, Adams DJ, Cannell M, Van Breemen C. Calcium-entry-dependent oscillations of cytoplasmic calcium concentration in cultured endothelial cell monolayers. *Proc Natl Acad Sci USA* 1992; **89**: 1690–1694.
 31. Pralong WF, Wollheim CB, Bruzzone R. Measurement of cytosolic free Ca^{2+} in individual pancreatic acini. *FEBS Lett* 1988; **242**: 79–84.
 32. Pickles RJ, Brayden DJ, Cuthbert AW. Synchronous transporting activity in epithelial cells in relation to intracellular calcium concentration. *Proc R Soc Lond [Biol]* 1991; **245**: 153–158.
 33. Boitano S, Dirksen ER, Sanderson MJ. Intercellular propagation of Ca^{2+} waves mediated by inositol trisphosphate. *Science* 1992; **258**: 292–295.
 34. Robb-Gaspers LD, Thomas AP. Coordination of Ca^{2+} signalling by intercellular propagation of Ca^{2+} waves in the intact liver. *J Biol Chem* 1995; **270**: 8102–8107.
 35. Sneyd J, Wetton BTR, Charles AC, Sanderson MJ. Intercellular calcium waves mediated by the diffusion of inositol trisphosphate: a two-dimensional model. *Am J Physiol* 1995; **268**: C1537–C1545.
 36. Berridge MJ. Inositol trisphosphate and calcium signaling. *Nature* 1993; **361**: 315–325.
 37. Ribalet B, Beigelmann PM. Calcium action potentials and potassium permeability activation in pancreatic β -cells. *Am J Physiol* 1980; **239**: C124–C133.
 38. Stojilkovic SS, Katt KJ. Calcium oscillations in anterior pituitary cells. *Endocr Rev* 1992; **13**: 256–280.
 39. Mealing G, Morley P, Whitfield JF, Tsang BK, Schwartz J-L. Granulosa cells have calcium-dependent action potentials and a calcium-dependent chloride conductance. *Pflügers Arch* 1994; **428**: 307–314.
 40. Klöckner U, Isenberg G. Calcium channel current of vascular smooth muscle cells: extracellular protons modulate gating and single channel conductance. *J Gen Physiol* 1994; **103**: 665–678.
 41. Alonso MT, Sanches A, Garcia-Sancho J. Monitoring of the activation of receptor-operated calcium channels in human platelets. *Biochem Biophys Res Commun* 1989; **162**: 24–29.
 42. Huerta M, Stefani E. Calcium action potentials and calcium currents in tonic muscle fibres of the frog (*Rana pipiens*). *J Physiol* 1986; **372**: 293–301.
 43. Nilius B, Kitamura K, Kuriyama H. Properties of inactivation of calcium channel currents in smooth muscle cells of rabbit portal vein. *Pflügers Arch* 1994; **426**: 239–246.
 44. Penner R, Fasolato C, Hoth M. Calcium influx and its control by calcium release. *Curr Opin Neurobiol* 1993; **3**: 368–374.